Realization and Evaluation of an Instructor-Like Assistance System for Collision Avoidance

Keji Chen, Takuma Yamaguchi, Hiroyuki Okuda, *Member, IEEE*, Tatsuya Suzuki, *Member, IEEE*, and Xuexun Guo

***Abstract*— Advanced driver assistance systems should not only make the driving experience safer and more comfortable, it should also have a positive effect on driving behaviors. In this paper, an instructor-like assistance system for collision avoidance is developed and realized on an actual vehicle. The proposed system is activated only if the driver is not operating the vehicle properly when facing a collision risk. The vehicle control is shared by the driver and the assistance system. It is controlled by servomotors. In order to fulfill this requirement, a constraint satisfaction problem (CSP) is proposed and solved based on safe driving constraints and predictive vehicle states. Vehicle motion is predicted by a combination of a dynamics model and a potential field model that reflects the driver's risk feeling to an obstacle. Improved driving behavior is verified and evaluated quantitatively based on driving simulator data. By comparing the driving data before and after using the assistance system, it is found that distance is increased and speed is reduced when passing an obstacle. As a result, driving behavior becomes safer for collision avoidance due to the system's instruction. Furthermore, an experiment with an actual vehicle also demonstrates the practicability of the control system and shows the influence of different safe driving constraints.**

***Index Terms*— Advanced driver assistance systems, intelligent vehicles, collision avoidance.**

I. Introduction

DUE to the remarkable development of sensor technologies and artificial intelligence, it is likely that high level autonomous driving will be available in the near future. However, there is still a long way to go before a completely trustworthy autonomous driving system is designed. Moreover, advanced driver assistance systems (ADAS) have not been widely implemented thus far. Therefore, human-centered ADASs, where human drivers are responsible, are still worth designing and developing.

Manuscript received April 17, 2019; revised September 15, 2019, December 16, 2019, and January 25, 2020; accepted February 10, 2020. This work was supported in part by the Japan Science and Technology Agency (JST) through the Center of Innovation Program (Nagoya-COI). The work of Keji Chen was supported by the China Scholarship Council (No. 201706950050). The Associate Editor for this article was L. Li. *(Corresponding author: Keji Chen.)*

Keji Chen is with the School of Automotive Engineering, Wuhan University of Technology, Wuhan 430070, China, and also with the Graduate School of Engineering, Nagoya University, Nagoya 4648603, Japan (e-mail: studentabc@126.com).

Takuma Yamaguchi, Hiroyuki Okuda, and Tatsuya Suzuki are with the Graduate School of Engineering, Nagoya University, Nagoya 4648603, Japan (e-mail: t_yamaguchi@nuem.nagoya-u.ac.jp).

Xuexun Guo is with the School of Automotive Engineering, Wuhan University of Technology, Wuhan 430070, China (e-mail: guoxx@whut.edu.cn).

Digital Object Identifier 10.1109/TITS.2020.2974495

For drivers with good driving skills, inattention may be caused by fatigue or using a cell phone. On the other hand, for drivers with poor skills, such as new drivers and elderly drivers, driving risks may be due to misjudgments and delayed response time. To address these issues, ADASs, such as collision warning/avoidance systems, play important roles in alerting drivers or taking action when there is no response from drivers [1]. Some studies have reviewed and classified ADASs according to their functions and have concluded that such systems have a positive impact on road safety and traffic efficiency [2]. In addition to providing real-time support in dangerous situations, ADASs can improve driving behavior. Driving behavior could become safer and more efficient under the influence of an ADAS, particularly for elderly and inexperienced drivers [3]. Heijer *et al.* also found that implementation of an ADAS will improve driving skills, and, more importantly, the improvement will maintain even if the system fails [4].

Various brake assistance systems have been developed for rear-end collision mitigation. The Volvo Car Corporation has developed an automatic emergency braking system with pedestrian detection. The system can quickly provide full braking power to avoid accidents in urban environments [5]. In addition, adaptive cruise control and forward collision warning/avoidance have been integrated in a longitudinal driving assistance system [6]. Active front steering is also extensively exploited in collision avoidance systems. Model predictive control (MPC) has been proposed for active steering control, and collision avoidance maneuvers were tested on icy roads [7]. An evasive trajectory method, wherein feedback approaches are utilized for lateral control, has been designed for obstacle avoidance [8]. These ideas of active front steering basically make the vehicle track a collision-free path.

In some driver assistance systems for lane departure avoidance, the system will take over if driver inattentiveness as well as the risk of lane departure are found. For such systems, methods to switch between the driver and the system have been studied [9]–[11]. Different collision avoidance methods have been proposed for unmanned aerial vehicles (UAV) or mobile robots. Jenie *et al.*. combined the velocity obstacle method with a sense and avoid system for UAV collision avoidance. In that study, the probability of a collision map is analyzed [12]. Additionally, Jin *et al.* presented a good idea to solve the obstacle avoidance problem of mobile robots that included a mechanism to switch the system between autonomous control and teleoperation mode [13]. However,

for passenger vehicles, sometimes allowing a system that is not sufficiently reliable to take control may not be acceptable, particularly when the shifting timing to the system is counter to driver intentions. Shared control, where an assistance system and a driver control the vehicle concurrently, have been proposed to improve acceptance of ADASs [14]. A cooperative strategy between a human driver and the system that uses the weighting function of a Gaussian distribution has been designed [15]. Rather than simply mixing driver and controller commands, a method that incorporates the driver commands directly into the MPC formulation has been proposed [16].

Acceptance of ADASs is increasing; however, as outlined in a previous study [17], the assistance is often poorly understood by users. In other words, drivers may feel strange or uncomfortable even if the system's action is acceptable. Typically, human drivers do not always follow a certain path. Instead, drivers select a safe driving area. Consequently, researchers have paid more attention to constraint-based methods or envelope-based methods. A potential elastic band model was presented to calculate an appropriate driving corridor for avoiding obstacles [18]. Anderson *et al.* designed safe homotopies where the driver can operate freely without any intervention and utilized MPC to ensure the vehicle did not violate safety constraints [19]. Similarly, Erlien *et al.* proposed applying the MPC framework for obstacle avoidance and stability control using safe driving envelopes. One envelopes is defined by the vehicle handling limits, and the other is based on the environmental constraints [20], [21]. These approaches imply that, when the driver shares the same driving envelope with the assistance system, cooperation will function harmoniously. Nevertheless, the assistance may still be undesirable if the driver and the assistance system cannot share the same envelope. The inability to share the same envelope is caused by incongruence between the driving characteristic expressed by a cost function in the control system and the original one of the driver. To cope with this problem, driver models that employ personal driving data are presented to predict drivers' behaviors and make the assistance control follow their habits and characteristics [22]–[24].

The control scheme presented in this paper combines the advantages of shared control and constraint-based methods. Steering and braking control is shared by the driver and the assistance system; however, the assistance system will not override human control. Moreover, the assistance control will only be activated if the predictive vehicle states violate the safety constraints. In addition, the proposed assistance system can also function as a driving instructor to improve driving behavior. The constraints are expressed by a safe driving region and a limitation on vehicle speed, and the vehicle motion prediction is computed using a driver-vehicle model. Based on the constraints and the predictive model, a constraint satisfaction problem (CSP) is solved to obtain the safe range of steer angles and longitudinal acceleration. Two types of experiments are designed and conducted based on a driving simulator and a real vehicle. Servomotors are used for assistant control operations, and multimodal visual warning is also designed. The driving simulator experiment verifies that the driver's inherent characteristics are improved by comparing the driving data before and after experiencing the proposed assistance system. The real vehicle experiment was conducted primarily to verify the practicability of the system on an actual vehicle and to show the influence of different safe driving constraints.

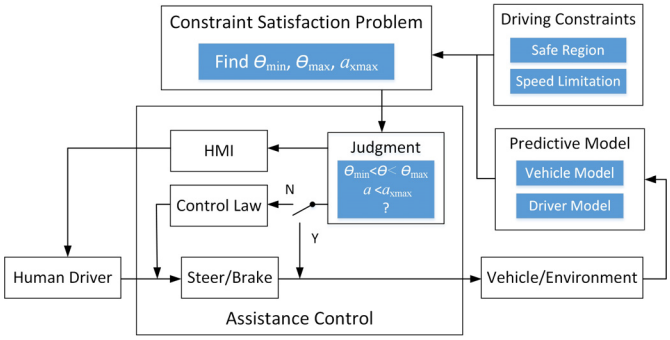

Fig. 1. Framework of the instructor-like assistance control system.

In summary, the primary contributions of this paper are as follows. (1) A new predictive model of vehicle motion is built. (2) A more efficient search algorithm for CSP is proposed. (3) Experimental results demonstrate that safety in real-time driving and improved driving behavior has been achieved simultaneously.

The remainder of this paper is organized as follows. The architecture of the instructor-like assistance system is presented in Section II. The expressions for the safety constraints and the driver-vehicle model are given in Section III. The CSP and the control law are presented in Section IV. In Section V, driving behavior improvement is verified. The real vehicle test and results are discussed in Section VI. The conclusions and suggestions for future work are presented in Section VII.

II. Overview of Assistance System

The overall architecture of the proposed system primarily comprises driving constraints, the predictive model, the CSP, and an assistance control module. As mentioned previously, the objective of the assistance system is to correct the driver's inappropriate driving behavior so as not to violate the safety constraints over the prediction horizon. The control flow is presented in Fig. 1.

The predictive model combines a vehicle model and a driver model that adopts the potential field method to capture driver characteristics relative to obstacle avoidance. The driving constraints consider two aspects of driving safety, i.e., lateral safety and longitudinal safety. For example, for driving on a straight road, lateral safety can be expressed by the maximum and minimum lateral positions that form a safe region. Longitudinal safety can be defined as the speed limit at which the vehicle should decelerate when passing an obstacle or going through an intersection.

However, only judging by the safe driving region and speed limit is not sufficient for implementation of the control system. The constraints should be converted to the range of the system input; thus, the CSP is proposed. By solving the CSP with the safety constraints and the predictive model, the safe range

of steering angles and longitudinal acceleration are obtained. Therefore, the assistance system is able to judge whether the current driving behavior will be safe in the future. If safe, the vehicle is completely controlled by the human driver; if dangerous, assistant steering or braking is added to the operation together with the human driver's operation, which is a type of shared control. In addition, the human–machine interface (HMI) for visual assistance is designed to warn the driver before the system has to intervene.

III. Safety Constraints and Vehicle-Driver Model

A. Safe Driving Region and Speed Limit

Unlike the driving envelope, which only considers environmental and vehicular factors [18]–[21], the safety constraints proposed in this paper also consider driver behaviors. Herein, the idea is to identify the constraint model using the driving data following previously proposed methods, e.g., the method proposed by Okuda *et al.* [22]. Note that constraint model identification is a difficult and complex topic and is beyond the scope of this paper. Herein, we assume the constraint model can be formulated as follows:

$$f_{\mathrm{b}}(x) = k_1 - k_3 \exp(-(x - (x_{\mathrm{ob}} - s))/k_2) \tag{1}$$

where k_1, k_2, and k_3 are parameters, x_{ob} is the longitudinal position of the obstacle, s is the offset, and (x, y) is vehicle position. Three types of constraints are applied in the system, $S_{\mathrm{ub}}(x)$, $S_{\mathrm{lb}}(x)$, and $V_{\mathrm{ub}}(x)$, which represent the upper bound of y, the lower bound of y, and the speed bound, respectively. We assume that $S_{\mathrm{ub}}(x)$, $S_{\mathrm{lb}}(x)$, and $V_{\mathrm{ub}}(x)$ can be expressed by $f_{\mathrm{b}}(x)$ with different parameters. These constraints indicate that, when approaching the obstacle, the ego car should steer away to avoid the collision and decelerate to mitigate risk. An example is given in Fig. 2, where the constraints, the allowed vehicle states, and the road environment are illustrated. The calculation of allowed vehicle states will be introduced in the following section. Ideally, the lateral position of the ego car should stay between $S_{\mathrm{ub}}(x)$ and $S_{\mathrm{lb}}(x)$, which is called the safe driving region, and vehicle speed should be less than $V_{\mathrm{ub}}(x)$.

Since we focus on the control strategy and its verification and evaluation in this paper, techniques for perception and identification of the obstacle are not discussed. Sensors, such as radar, lidar, and cameras, can be used to detect the obstacle. Currently, we simply assume that the obstacle is detected in advance. Then, the corresponding safety constraints are generated, as shown in Fig. 2.

Note that the assumed mathematical form of the constraints does not invalidate the assistance control but may affect comprehensibility for different drivers. The merits of using this function can be summarized in two points. One merit is to obtain the smooth bounds because the raw driving data may not be smooth. Smooth bounds will result in smooth control. The other is to make the bounds adjustable by changing the parameters for different driving scenarios. For example, if the width of road or the location of the obstacle changes, we can simply change the parameters in the function.

B. Simplified Dynamics Model

In this paper, the following reasonable assumptions are made: (1) the vehicle is a rigid body, (2) roll, pitch, and vertical motion are ignored, (3) the steering is bilateral symmetry, and (4) tire slip ratio and sideslip angle are very small. Therefore, the vehicle dynamics can be described based on the bicycle model as follows.

$$mv\dot{\beta} + 2(k_{\mathrm{f}} + k_{\mathrm{r}})\beta + (mv + 2(l_{\mathrm{f}}k_{\mathrm{f}} - l_{\mathrm{r}}k_{\mathrm{r}})/v)\dot{\varphi} = 2k_{\mathrm{f}}\delta \tag{2}$$

$$I_{\mathrm{z}}\dot{\omega} + 2(l_{\mathrm{f}}k_{\mathrm{f}} - l_{\mathrm{r}}k_{\mathrm{r}})\beta + 2(l_{\mathrm{f}}^2 k_{\mathrm{f}} + l_{\mathrm{r}}^2 k_{\mathrm{r}})\dot{\varphi}/v = 2l_{\mathrm{f}}k_{\mathrm{f}}\delta \tag{3}$$

Here, β is the slip angle, φ is the yaw angle, ω is the yaw rate, δ is the front steering angle, v is the longitudinal speed, m, I_{z}, v, l_{f}, l_{r}, k_{f}, and k_{r} are the mass of vehicle, the yaw moment of vehicle inertia, the longitudinal speed of the vehicle, the distance from the center of gravity (CG) to the front axle, the distance from the CG to the rear axle, the cornering stiffness of the front wheels, and the cornering stiffness of the rear wheels, respectively.

Assuming that the vehicle is in the steady-state circular and the slip angle is zero, the yaw rate can be simplified as follows.

$$\omega = v/(l_{\mathrm{f}} + l_{\mathrm{r}})\delta \tag{4}$$

Then, the vehicle speed predicted by the dynamics model is given as follows:

$$\boldsymbol{V}_{\mathrm{d}} = \begin{bmatrix} v\cos(\varphi + \omega) \\ v\sin(\varphi + \omega) \end{bmatrix} = \begin{bmatrix} V_{\mathrm{d,x}} \\ V_{\mathrm{d,y}} \end{bmatrix} \tag{5}$$

As a model predictive method, the accuracy of vehicle motion estimation should be guaranteed over the entire prediction horizon. Nevertheless, the vehicle dynamics model only has high accuracy in the short term because drivers' maneuvers may vary over time. As a result, the driver model, which is suitable for long term prediction by considering changes in driver maneuvers, is also considered.

C. Potential Field Model

In the driver model, driving behavior in collision avoidance is modeled by several potential field functions that represent both the road environment and the risk feeling of the driver. The potential functions are given for going forward U_{g}, side walls U_{w}, and the obstacle U_{ob}:

$$U_{\mathrm{g}}(x, y) = -w_{\mathrm{g}}x \tag{6}$$

$$U_{\mathrm{w}}(x, y) = w_{\mathrm{w}}(\exp(-(y - y_{\mathrm{wl}})^2/\sigma_{\mathrm{w}}^2) + \exp(-(y - y_{\mathrm{wr}})^2/\sigma_{\mathrm{w}}^2)) \tag{7}$$

$$U_{\mathrm{ob}}(x, y) = w_{\mathrm{ob}}\exp(-(x - x_{\mathrm{ob}})^2/\sigma_{\mathrm{x}}^2 - (y - y_{\mathrm{ob}})^2/\sigma_{\mathrm{y}}^2) \tag{8}$$

Here, x and y represent the position of vehicle, x_{ob} and y_{ob} represent the position of the obstacle, y_{wl} and y_{wr} represent the position of a wall, w_{g}, w_{w}, and w_{ob} are the weight parameters, and σ_{w}, σ_{x}, and σ_{y} are the standard deviations.

In the conventional potential method, these potential functions are only based on the geometric information of environmental elements. However, to increase the congruity between the driver and the system, the potential functions should be designed to reflect the risk feeling of the driver during

Algorithm 1: CSP A

Given:

1. $N \in \mathbb{N}$, number of prediction steps,
2. $\mathbf{N} = \{0, 1, \ldots, N\}$, set of prediction steps,
3. $S_{\mathrm{ub}}(x) \in \mathbb{R}$ and $S_{\mathrm{lb}}(x) \in \mathbb{R}$, lateral upper and lower bounds of the safety region at x,
4. $\hat{X}(t + i\,\Delta t|\theta(t)) \in \mathbb{R}$, $\hat{Y}(t + i\,\Delta t|\theta(t)) \in \mathbb{R}$, i-step-ahead predictive longitudinal and lateral position when the current steering angle is $\theta(t)$ at time t,

Find: $\boldsymbol{\theta} = [\theta_{\min}(t), \theta_{\max}(t)]$
which satisfies

$$S_{\mathrm{lb}}(\hat{X}(t + i\,\Delta t|\theta(t))) \leq \hat{Y}(t + i\,\Delta t|\theta(t))(\forall\theta(t) \in \boldsymbol{\theta}, \forall i \in \boldsymbol{N}) \quad (12)$$

$$\hat{Y}(t+i\,\Delta t|\theta(t)) \leq S_{\mathrm{ub}}(\hat{X}(t+i\,\Delta t|\theta(t)))(\forall\theta(t) \in \boldsymbol{\theta}, \forall i \in \boldsymbol{N}) \quad (13)$$

obstacle avoidance. Since the potential field model described by Equations (6–8) is a repulsive field, the repulsive force generated by the potential field can reflect the risk feeling of different drivers. For example, as the driver perceives more risk, the vehicle will be driven at a greater distance from the obstacle or wall. Therefore, we identify function parameters by observing the driving data to personalize the potential fields. The details of the parameter identification can be found in our previous paper [28]. Then, the vehicle speed, $V_{\mathrm{p,x}}$ and $V_{\mathrm{p,y}}$, in the x and y directions, respectively, based on the driver model can be calculated by taking the negative gradient of the potential functions.

$$\boldsymbol{V}_{\mathrm{p}} = -\nabla(U_{\mathrm{g}}(x, y) + U_{\mathrm{w}}(x, y) + U_{\mathrm{ob}}(x, y)) = \begin{bmatrix} V_{\mathrm{p,x}} \\ V_{\mathrm{p,y}} \end{bmatrix} \quad (9)$$

Finally, these two models can be combined as a vehicle-driver model to predict the future position of vehicle $(\hat{X}, \hat{Y})$ as follows:

$$\begin{bmatrix} \hat{X}(t + \Delta t) \\ \hat{Y}(t + \Delta t) \end{bmatrix} = \begin{bmatrix} \hat{X}(t) \\ \hat{Y}(t) \end{bmatrix} + \Delta t \cdot [(1-\alpha)\boldsymbol{V}_{\mathrm{p}}(\hat{X}(t), \hat{Y}(t)) + \alpha \boldsymbol{V}_{\mathrm{d}}(\delta(t))] \quad (10)$$

where t is current time, Δt is the time step, and α is a weighting coefficient that adjusts the weighting of the calculation of (5) and (9).

$$\alpha = c^i \quad (11)$$

Here, c is a constant between 0 and 1, and i is the prediction step. In the prediction horizon, α decreases monotonically so that the dynamics model is dominant in the short term while the driver model is increasingly more important in the long term.

IV. Constraint-Based Control Algorithm

A. CSP Solution

The CSP determines whether the predictive vehicle behavior satisfies the safety constraint. Its solution is given to the system as an admissible set of the driving maneuvers that ensure driving safety in the future. The driving maneuver is represented by a pair of steer angles θ and longitudinal acceleration a_{x}, and there is an affine relationship between θ and δ. Consequently, solving the CSP involves computing the admissible safety set $\theta_{\mathrm{safe}}(t) = [\theta_{\min}(t), \theta_{\max}(t), a_{\mathrm{xmax}}(t)]$ according to the constraints of the driving region and vehicle speed described in Section III A. Due to the model predictive method, it is expected that the assistance control is executed before the ego car gets too close to the obstacle.

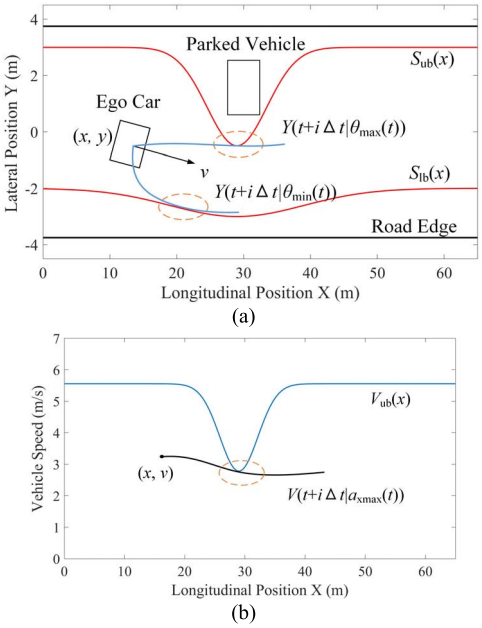

Fig. 2. Example of the relationship between driving constraints and vehicle predictive states; (a) safe driving region and (b) speed bound.

Figure 2 shows an example of the calculation of $\theta_{\min}(t)$ and $\theta_{\max}(t)$ in an avoidance task involving a parked car, where the safety region is represented as the limits of safety position $S_{\mathrm{ub}}(x)$ and $S_{\mathrm{lb}}(x)$ at position x. In this example, CSP A is formulated as a search problem of the admissible safety set of driving maneuver $\theta_{\min}(t)$, $\theta_{\max}(t) \in \boldsymbol{\Theta} = \{\theta_{\min}, \theta_{\min} + \Delta\theta, \ldots, \theta_{\max} - \Delta\theta, \theta_{\max}\}$, where $\theta_{\min}$, $\theta_{\max}$, and $\Delta\theta$ are the lower bounds, upper bounds, and resolution of the steering angle, respectively. Note that $\theta_{\min}$ and $\theta_{\max}$ are physical bounds of the steering angle (constant parameters), and are different from the admissible safety set at each time instant.

However, it can be observed that CSP A incurs significant computational costs due to the large search space defined by $\mathbf{N}\times\boldsymbol{\Theta}$. For example, if $|\boldsymbol{\Theta}| = 1000$ and $|\mathbf{N}| = 20$, the algorithm has to compute the predictive position of the vehicle and check the inequalities (12) and (13) 20000 times. To reduce the computational cost, the following assumption is introduced.

$$\text{If } \theta_1(t) \leq \theta_2(t), \quad \hat{Y}(t + i \cdot \Delta t\,|\theta_1(t)) \leq \hat{Y}(t + i \cdot \Delta t\,|\theta_2(t))(\forall i \in \mathbf{N}) \quad (14)$$

This assumption implies that the magnitude relation of $\hat{Y}(t+i\,\Delta t|\theta(t))$ for different $\theta(t)$ is invariant over the prediction horizon. Therefore, solving the safety constraints $\theta_{\min}(t)$ and

$\theta_{\max}(t)$ is equivalent to finding the vehicle's lateral position that contacts the driving bounds $S_{\text{ub}}(x)$ and $S_{\text{lb}}(x)$, as shown in Fig. 2. The assumption (14) is satisfied when the parameter c in (11) is close to 1 so that the vehicle dynamics model can be more dominant in the prediction [24].

Algorithm 2: CSP B

Given:
The same as CSP A;
Find: $\theta_{\min}(t)$, $\theta_{\max}(t)$
which satisfies

$$S_{\text{lb}}(\hat{X}(t+i\,\Delta t|\theta_{\min}(t))) \le \hat{Y}(t+i\,\Delta t|\theta_{\min}(t))(\forall i \in \mathbf{N}) \quad (15)$$

$$\hat{Y}(t+i\,\Delta t|\theta_{\max}(t)) \le S_{\text{ub}}(\hat{X}(t+i\,\Delta t|\theta_{\max}(t)))(\forall i \in \mathbf{N}) \quad (16)$$

Pseudo-code

for searching $\theta_{\max}$

1. Set $\theta_{\text{u}} = \theta_{\max}$, $\theta_{\text{l}} = \theta_{\min}$, $\theta_{\max} = (\theta_{\text{u}} + \theta_{\text{l}})/2$;
2. If the inequality (16) holds, then set $\theta_{\text{l}} = \theta_{\max}$, else set $\theta_{\text{u}} = \theta_{\max}$;
3. Set $\theta_{\max} = (\theta_{\text{u}} + \theta_{\text{l}})/2$;
4. If $(\theta_{\text{u}} - \theta_{\text{l}}) \le \Delta\theta$, then terminate the algorithm, else go to step 2.

Pseudo-code

for searching $\theta_{\min}$

1. Set $\theta_{\text{u}} = \theta_{\max}$, $\theta_{\text{l}} = \theta_{\min}$, $\theta_{\min} = (\theta_{\text{u}} + \theta_{\text{l}})/2$;
2. If the inequality (15) holds, then set $\theta_{\text{u}} = \theta_{\min}$, else set $\theta_{\text{l}} = \theta_{\min}$;
3. Set $\theta_{\min} = (\theta_{\text{u}} + \theta_{\text{l}})/2$;
4. If $(\theta_{\text{u}} - \theta_{\text{l}}) \le \Delta\theta$, then terminate the algorithm, else go to step 2.

Based on the assumption (14), CSP A can be reformulated as the CSP B. Any $\theta(t) \in [\theta_{\min}(t), \theta_{\max}(t)]$, where $\theta_{\min}(t)$ and $\theta_{\max}(t)$ are the solutions of CSP B, will satisfy the inequalities (15) and (16). Therefore, the admissible safety set of steer angles is derived if only CSP B is solved.

Although the discussion above is related to steering angles, the CSP for vehicle speed is formulated in the same way. The constraint of a_{x} is obtained by solving CSP C according to the speed bound $V_{\text{ub}}(x)$, as shown in Fig. 2.

CSPs B and C can be solved using the binary search method. Note that pseudocode for CSPs B and C is given above. Thanks to the binary search method, the required computational cost is reduced to $O(2|\mathbf{N}|\log_2|\Theta|)$. For example, if $|\Theta| = 1000$ and $|\mathbf{N}| = 20$, the number of iterations is only 400, which is much smaller than the number of iterations required by the first algorithm (CSP A). As a result, the constraints for safe driving are available in real-time.

B. Control Law

After solving the CSP, the system will supervise the driving maneuver so that, if $[\theta(t), a_{\text{x}}(t)]$ exceeds the safety set $\theta_{\text{safe}}(t) = [\theta_{\min}(t), \theta_{\max}(t), a_{\text{xmax}}(t)]$, assistance control will be activated such that the vehicle states return to safe regions.

Algorithm 3: CSP C

Given:
1. $N \in \mathbb{N}$, number of prediction steps,
2. $\mathbf{N} = \{0, 1, \ldots, N\}$, set of prediction steps,
3. $V_{\text{ub}}(x) \in \mathbb{R}$, upper bounds of vehicle speed at x,
4. $\hat{V}(t + i\,\Delta t|a_{\text{x}}(t)) \in \mathbb{R}$, i-step-ahead predictive vehicle speed
when the current acceleration is $a_{\text{x}}(t)$ at time t;

Find: $a_{\text{xmax}}(t)$
which satisfies

$$\hat{V}(t+i\,\Delta t|a_{\text{xmax}}(t)) \le V_{\text{ub}}(\hat{X}(t+i\,\Delta t|\theta(t)))(\forall i \in \mathbf{N}) \quad (17)$$

Pseudo-code

for searching a_{xmax}

1. Set $a_{\text{u}} = A_{\max}$, $a_{\text{l}} = A_{\min}$, $a_{\text{xmax}} = (A_{\max} + A_{\min})/2$;
2. If the inequality (17) holds, then set $a_{\text{l}} = a_{\text{xmax}}$, else set $a_{\text{u}} = a_{\text{xmax}}$;
3. Set $a_{\text{xmax}} = (a_{\text{u}} + a_{\text{l}})/2$;
4. If $(a_{\text{u}} - a_{\text{l}}) \le \Delta a_{\text{x}}$, then terminate the algorithm, else go to step 2.

The control law for steering and brake assistance is designed as follows.

$$\tau = \begin{cases} D_{\text{s}}\dot{\theta} + K_{\text{s}}(\theta - \theta_{\max}) & \text{if } \theta \ge \theta_{\max} \\ 0 & \text{else if } \theta_{\max} > \theta > \theta_{\min} \\ D_{\text{s}}\dot{\theta} + K_{\text{s}}(\theta - \theta_{\min}) & \text{else if } \theta \le \theta_{\min} \end{cases} \quad (18)$$

$$p_{\text{b}} = \begin{cases} K_{\text{b}}(a_{\text{x}} - a_{\text{xmax}}) & \text{if } a_{\text{x}} \ge a_{\text{xmax}} \\ 0 & \text{otherwise} \end{cases} \quad (19)$$

where τ is the additional steering torque, p_{b} is the percentage of brake pedal travel, D_{s} and K_{s} are the steering assistant control parameters, and K_{b} is the brake assistance control parameter. For safety reasons, the maximum values of τ and p_{b} are set to 0.4 Nm and 30%, respectively. Note that the control law is designed for driver assistance rather than for an autonomous driving system that controls the vehicle such that it follows a planned path [26]–[29]. In other words, in this control framework, the human driver is responsible for controlling the vehicle not the proposed assistance system.

V. Verification of Driving Behavior Improvement

As mentioned previously, the system is developed for both collision avoidance and driving guidance, which should have a positive effect on driving behavior. Thus, an experiment based on a driving simulator was designed and conducted to verify the improvement of collision avoiding behavior. The configuration of the driving simulator is presented in Fig. 3(a). It is based on a PC and display monitors; however, the driver's seat, steering wheel, and pedals are actual parts from a Toyota Prius. The controlled vehicle in the visual environment is simulated by CarSim. Additionally, the driver can get feedback from the LED lights on the steering wheel, the motor in the steering shaft, and the vibration device attached to the pedal.

The margin and vehicle speed when passing by the parked vehicle are used to characterize the collision avoiding behavior,

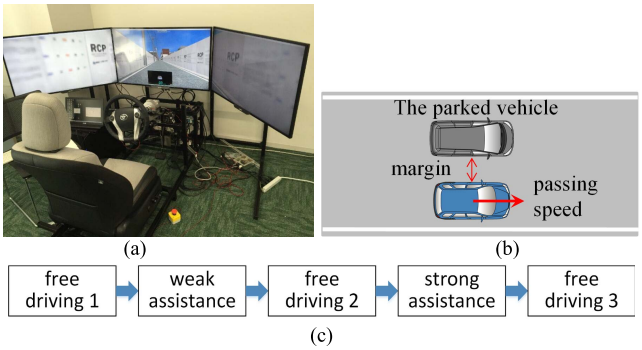

Fig. 3. Experimental plan with the driving simulator; (a) configuration of driving simulator, (b) collected data, (c) test procedure.

TABLE I
AVERAGE RESULTS OF THE TEST ON THE DRIVING SIMULATOR

Procedure	Margin (m)	Passing speed (km/h)	Acceptance scores
free driving 1	0.712	42.81	/
weak assistance	0.758	28.46	3.69
free driving 2	0.735	38.42	/
strong assistance	0.812	20.91	3.44
free driving 3	0.781	33.26	/

as shown in Fig. 3(b). In general, a Japanese driving instructor will teach novice drivers to be cautious of door opening of a parked vehicle and be aware of the blind area behind the vehicle. In this case it is safer if the margin is larger and the speed is lower when passing the obstacle because someone may come out of the shadow of the obstacle. The larger margin and lower speed will effectively reduce the risk or mitigate the collision.

Twenty-six men and women who had Japanese driving licenses participated in the experiment. The participants were asked to avoid a parked vehicle in an urban residential environment. The experiment proceeded in five steps, as shown in Fig. 3(c). Here, "free driving" means driving without assistance control and "weak/strong assistance" means driving with assistance of a larger or smaller safety region. The goals of these steps are explained as follows. (1) Free driving 1 is simply the initial driving. Here, the data are used to represent the original driving behavior. (2) Driving with weak/strong assistance shows system performance. (3) Free driving 2 and 3 evaluate the improvement of driving behavior due to the guidance of the proposed system. For each step, the participants were asked to drive three times after two trials, and the average margin and passing speed were collected for analysis. In addition, a questionnaire in which the participants graded the performance of the assistance system was administered to evaluate acceptance of the assistance. For example, participants were asked to describe their satisfaction with the assistance system by assigning scores between 0 and 5. The methods used to evaluate and analyze the questionnaire were adopted from a previous study [33].

The results for average margin are presented in Fig. 4 and the results for speed are given in Fig. 5. The figures show the

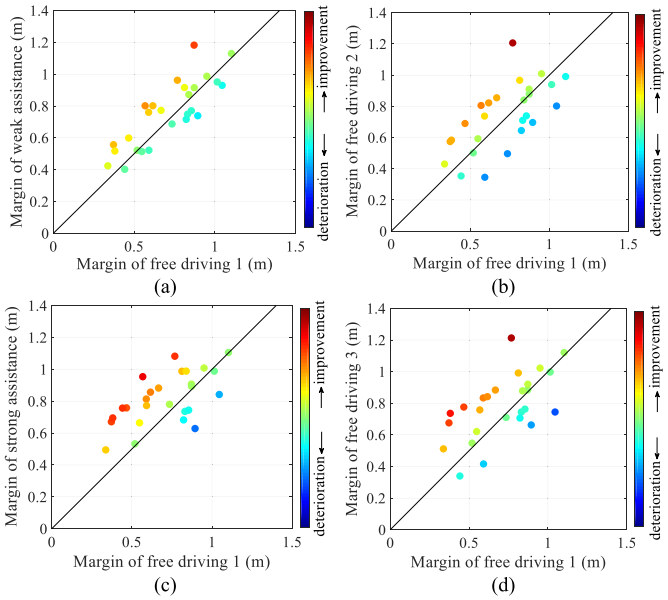

Fig. 4. Margin compared with free driving 1; (a) with weak assistance, (b) free driving 2, (c) with strong assistance, (d) free driving 3.

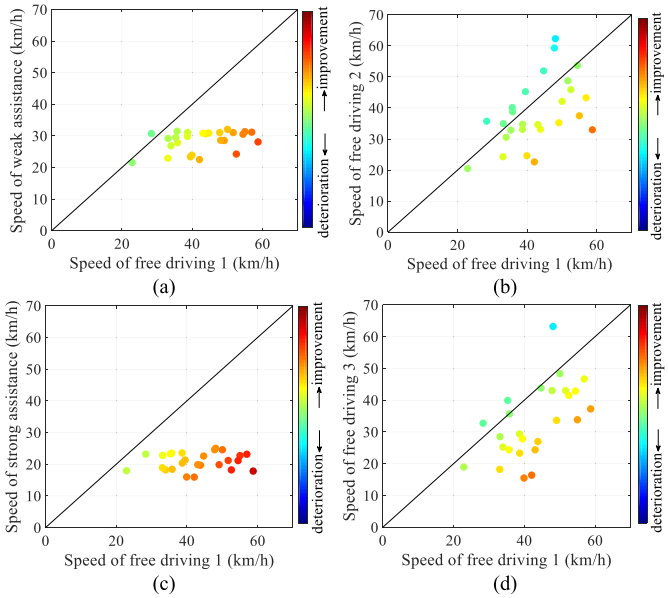

Fig. 5. Speed compared with free driving 1; (a) with weak assistance, (b) free driving 2, (c) with strong assistance, (d) free driving 3.

change of driving behavior by comparing the other results to the free driving 1 results, i.e., the initial and original driving behavior. The average margin and speed of all participants are summarized in Table I.

In general, the improvement of driving behavior can be represented by the increasing margin and decreasing speed compared with the initial driving behavior. As can be seen in Figs. 4(a) and (c), the margin with weak and strong assistance increased for most part, i.e., precisely 6.4% and 14.0% mean increase, respectively. Due to the intervention of the assistance control system, speed decreased dramatically, i.e., 33.5% and 51.2% on average, as shown in Figs. 5(a) and (c), respectively. More importantly, solid evident of the positive

TABLE II
SYSTEM PARAMETERS

Parameter	Value
l_f	0.82
l_r	0.71
w_g	3.05
w_w	8.57
w_{ob}	6.31
σ_w	2.87
σ_x	32.04
σ_y	5.34
Δt	0.1s
c	0.98
D_s	0.01
K_s	0.382
K_b	0.5

effect on driving behavior is shown in Figs. 4(b) and (d) and Figs. 5(b) and (d). Although the assistance system is turned off, the average margin still increased by 3.2% and 9.7% after the participants experience weak and strong assistance, respectively. Furthermore, the remarkable decrease of the passing speed can be observed in Figs. 5(b) and (d), where the average reduced rates are 10.3% and 22.3%, respectively. Therefore, from the analysis above, it can be concluded that the driver's inherent characteristic is improved after experiencing the proposed assistance system.

Furthermore, as shown in Table I, the acceptance score for weak assistance is lower than the score for strong assistance. This result indicates that stronger assistance may reduce acceptance in spite of resulting in safer driving behavior. Therefore, the tradeoff between the strength and acceptance of the system should be considered seriously when designing the assistance control.

VI. REAL VEHICLE EXPERIMENT

A. Experimental Setting

The applicability of the system was also tested on a small electric vehicle at low speed. More critical collision avoidance maneuvers at higher speed are not suitable for our experimental conditions at this time. In the current condition, it is difficult to have a significant number of test drivers perform the real vehicle experiment. Therefore, the system was tested by one driver who had experience driving an intelligent vehicle. However, this driver did not know the purpose of our research. The driver had five practices runs prior to the formal test.

In this experiment, the environment was a one-way road with a vehicle parked on the left side. The road is assumed to be 7 m ($y_{wl} = 3.5$ m, $y_{wr} = -3.5$ m) wide. The parked vehicle, which is regarded as the obstacle, is 4.8 m×1.84 m and located at $(x_{ob}, y_{ob}) = (40$ m, 2 m). The other parameters used in the system are listed in Table II with their values.

The vehicle states, such as position and orientation are measured by the RTK-GNSS (Oxford Technical Solutions, RT3002), as shown in Fig. 6(b), and the signal of steering

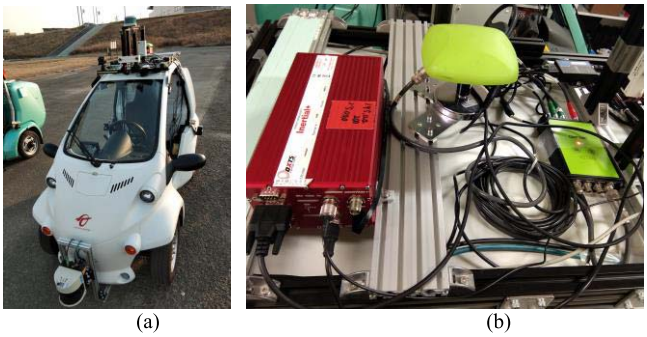

(a) (b)

Fig. 6. Test vehicle with the experimental equipment; (a) small electrical vehicle, (b) GPS and IMU.

TABLE III
CONSTRAINT FUNCTION PARAMETERS

$f_b(x)$	k_1	k_2	k_3	s
$S_{lb}(x)$	-2	200	1	3
$S_{ub1}(x)$	3	100	4	3
$S_{ub2}(x)$	2.5	100	3	3
$V_{ub1}(x)$	5.56	50	2.78	2
$V_{ub2}(x)$	8.33	50	4.17	2

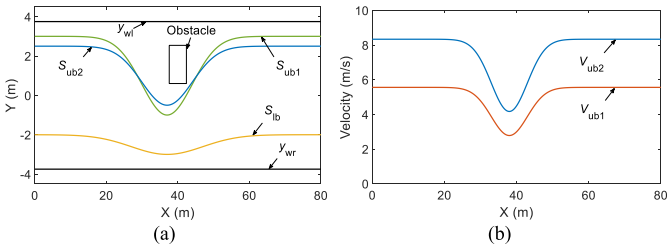

(a) (b)

Fig. 7. Driving constraints designed for the test, (a) safe driving region, (b) speed bound.

angle is obtained through the CAN. In addition, the steering and brake assistance control actions are realized by the servomotors attached to the steering shaft and brake pedal, respectively. The software is integrated in a PC (Intel Core i7-4790S 3.2GHz CPU) in the vehicle's trunk.

To evaluate the assistance system under different conditions, three combinations of constraints were implemented in the experiment. S_{ub1}, S_{lb}, and V_{ub1} are applied in Test A; S_{ub2}, S_{lb}, and V_{ub1} in Test B; and S_{ub2}, S_{lb}, and V_{ub2} in Test C. The parameters of the function for these constraints are given in Table III and illustrated in Fig. 7. As can be seen in the figure, compared with S_{ub2}, S_{ub1} makes the safe driving region wider at the beginning but narrower when passing by the obstacle. However, the variation of S_{ub2} is a little milder than that of S_{ub1}. In addition, on the whole, V_{ub2} is bigger than V_{ub1}.

B. Visual Warning

It is important to warn the driver before the assistance control is executed because sudden activation may surprise and distract the driver. The LED indicator is implemented as the HMI under the front windshield of the test vehicle, as shown

Fig. 8. LED on mode 0 under the front windshield of the test vehicle.

TABLE IV
MEANING OF THE LED MODES

Color and movement of LED	Meaning	Mode
Normal green	Safe	0
Normal red	Need to brake	1
Green left waving	Need to turn left	2
Red left waving	Need to brake and turn left	3
Green right waving	Need to turn right	4
Red right waving	Need to brake and turn right	5

in Fig. 8. The color and movement of the LED change to indicate different warning modes. To make the HMI easy to understand, we designed six warning modes numbered 0–5, as listed in Table IV.

Warning timing is a complicated issue that has been investigated previously [31], [32]. In this study, the warning trigger condition is simply derived from the condition in the control law, and it is ensured that the warning comes before the control operation. As a result, if the driver responds to the warning quickly, the assistance control may not intervene; otherwise, the system will control the vehicle concurrently with the driver.

C. Results and Discussions

The results of Test A, Test B, and Test C are shown in Figs. 9, 10, and 11, respectively. Except for the steering/brake assistance control, the results of the LED warning (Table IV) are also presented. Note that the label "assistant torque" means extra steering torque generated by the motor, and the label "assistant brake" means the percentage of brake pedal travel due to the proposed system.

In Test A, the assistant steering torque is given at approximately X = 20 to 30 m, where the steering angle exceeds $\theta_{\max}$, to help the vehicle turn a little more to the right. After overtaking the obstacle, the system no longer intervenes with human driving. The brake assistance is activated at approximately X = 20 to 35 m to make sure that the vehicle passes by the obstacle slowly. In addition, the LED warns the driver correspondingly. For example, from approximately X = 20 to 30 m, the LED mode is 5, which indicates that the vehicle should steer right and slow down simultaneously. Since the warning comes before the control, the driver could be well prepared for the assistance.

Compared to Test A, the upper bound of y is changed to S_{ub2} in Test B, where the safe driving region near the obstacle becomes a little larger. As shown in Fig. 10(a), the assistance

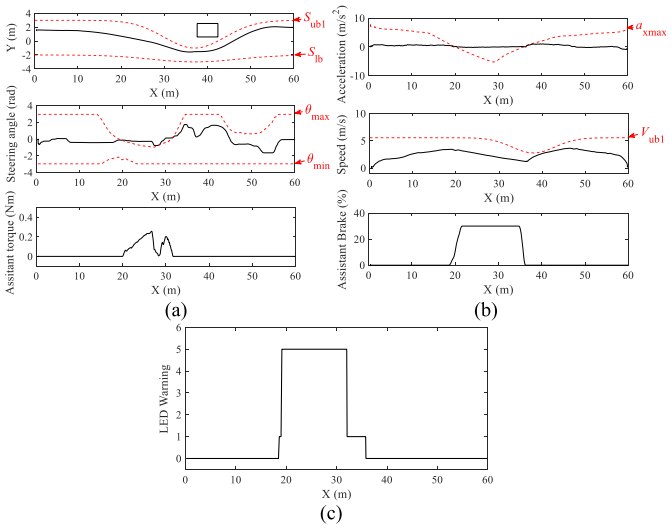

Fig. 9. Results of the instructor-like assistance control in Test A. (a) Steering assistance control, (b) brake assistance control, (c) LED warning.

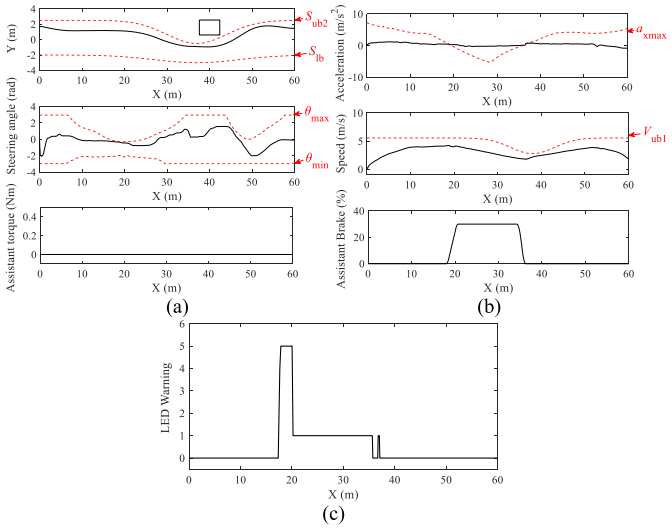

Fig. 10. Results of the instructor-like assistance control in Test B; (a) steering assistance control, (b) brake assistance control, (c) LED warning.

system allows the ego car to go by the obstacle at a closer distance compared to the trajectory in Fig. 9(a). Because the steering angle is always between $\theta_{\min}$ and $\theta_{\max}$, the assistant torque is not generated by the control system. However, the LED warning still reminds the driver to steer right at approximately X = 20 because the steering angle almost reaches $\theta_{\max}$. As expected, the assistance control decelerates the ego car until the vehicle is traveling sufficiently slowly to pass the obstacle safely.

Compared to Test B, in Test C the speed bound is changed to V_{ub2} from V_{ub1}. As a result, the driver may drive the vehicle at higher speed without the control system intervening. As shown in Fig. 11(b), the longitudinal acceleration is always less than the constraint; therefore, there is no assisted brake and the speed is entirely controlled by the driver. From Fig. 11(a), it is evident that the avoidance maneuver becomes worse than that in Tests A and B because the vehicle speed becomes

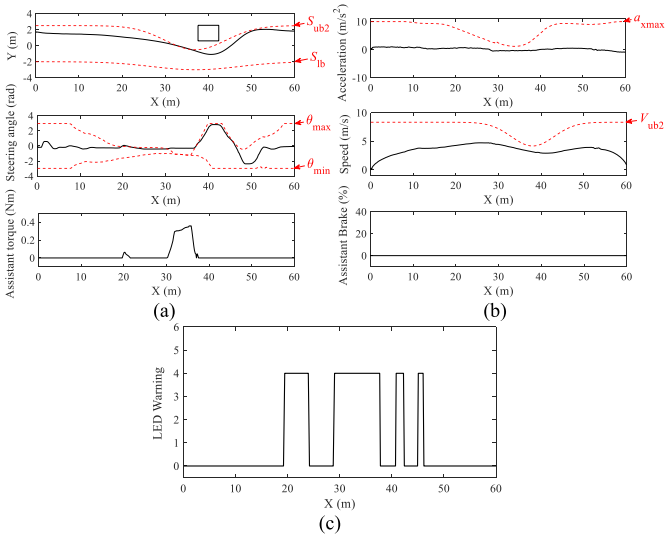

Fig. 11. Results of the instructor-like assistance control in Test C; (a) steering assistance control, (b) brake assistance control, (c) LED warning.

higher. Consequently, the assistant steering torque is greater, approximately X = 30 to 37 m, and the vehicle moves out of the safe driving region slightly. Moreover, the LED warning also helps the driver operate the vehicle within the safe driving region.

In summary, the test results reflect the characteristic of the proposed assistance system, i.e., assistance is provided only if necessary according to the prediction of vehicle motion. Moreover, the driving constraints significantly affect the driving behaviors of the ego car. For example, a low bound for speed is favorable for avoidance maneuvers. Furthermore, the experimental results showed no unstable system behavior.

VII. Conclusion

In this paper, an instructor-like assistance control system for collision avoidance is developed and tested on a real vehicle. The primary contributions of this paper are as follows. (1) An innovative motion prediction method that combines a simplified dynamics model and a potential field model are proposed. (2) A more efficient binary search algorithm is proposed to solve the CSP. (3) Two types of experiment are designed and conducted to show the significance of the developed control system. Improvement of a driver's inherent collision avoiding behavior is verified and evaluated based on driving simulator data. The positive effect of the assistance system is shown by the increase of margin and the reduction of passing speed. The real vehicle experiment also proved that the proposed system is practicable to assist the driver to avoid collision or mitigate risk. The assistance is given only when the driver fails to operate the vehicle safely; otherwise, the system will not distract the human driver.

It should be pointed out that a rigorous stability analysis is not given in this paper. In order to check stability, the dynamics of the vehicle and the operational characteristics of the human driver must be considered explicitly. Analysis and modeling of the human driver's operational characteristics is an independent research topic; thus, we intend to consider the stability issue in future work. In addition, we will also investigate the method used to build the constraint model, and the application of the proposed system will be extended to more complex driving conditions.

Acknowledgment

The authors would like to acknowledge Mr. H. Chin and Mr. R. Torii for their help with the experiment.

References

[1] J. Piao and M. McDonald, "Advanced driver assistance systems from autonomous to cooperative approach," *Transp. Rev.*, vol. 28, no. 5, pp. 659–684, Sep. 2008.

[2] J. Golias, G. Yannis, and C. Antoniou, "Classification of driver-assistance systems according to their impact on road safety and traffic efficiency," *Transp. Rev.*, vol. 22, no. 2, pp. 179–196, Jan. 2002.

[3] N. Congress, "The automated highway system: An idea whose time has come," *Public Roads*, vol. 58, no. 1, pp. 1–7, 1994.

[4] T. Heijer *et al.*, "Problem identification, user needs and inventory of ADAS," ADVISORS Project Deliverable D1/2.1, 2000.

[5] E. Coelingh, A. Eidehall, and M. Bengtsson, "Collision warning with full auto brake and pedestrian detection—A practical example of automatic emergency braking," in *Proc. IEEE 13th Int. Conf Intell. Transp. Syst.*, Madeira Island, Portugal, Sep. 2010, pp. 155–160.

[6] J. Wang, L. Zhang, D. Zhang, and K. Li, "An adaptive longitudinal driving assistance system based on driver characteristics," *IEEE Trans. Intell. Transp. Syst.*, vol. 14, no. 1, pp. 1–12, Mar. 2013.

[7] P. Falcone, F. Borrelli, J. Asgari, H. E. Tseng, and D. Hrovat, "Predictive active steering control for autonomous vehicle systems," *IEEE Trans. Control Syst. Technol.*, vol. 15, no. 3, pp. 566–580, May 2007.

[8] R. Isermann, M. Schorn, and U. Stählin, "Anticollision system PRORETA with automatic braking and steering," *Vehicle Syst. Dyn.*, vol. 46, pp. 683–694, Sep. 2008.

[9] N. M. Enache, S. Mammar, S. Glaser, and B. Lusetti, "Driver assistance system for lane departure avoidance by steering and differential braking," *IFAC Proc. Volumes*, vol. 43, no. 7, pp. 471–476, Jul. 2010.

[10] N. M. Enache, S. Mammar, M. Netto, and B. Lusetti, "Driver steering assistance for lane-departure avoidance based on hybrid automata and composite Lyapunov function," *IEEE Trans. Intell. Transp. Syst.*, vol. 11, no. 1, pp. 28–39, Mar. 2010.

[11] A. B. Neto, S. Scalzi, S. Mammar, and M. Netto, "Dynamic controller for lane keeping and obstacle avoidance assistance aystems," in *Proc. IEEE 13th Int. Conf Intell. Transp. Syst.*, Madeira Island, Portugal, Sep. 2010, pp. 1363–1368.

[12] Y. I. Jenie, E.-J. Van Kampen, C. C. de Visser, and Q. P. Chu, "Velocity obstacle method for non-cooperative autonomous collision avoidance system for UAVs," in *Proc. AIAA Guid., Navigat. Control Conf.*, Annapolis, MD, USA, Jan. 2014, pp. 1472–1483.

[13] J. Jin, N. Gans, Y. Kim, and S. Wee, "A switched-system approach to shared robust control and obstacle avoidance for mobile robots," in *Proc. ASME DSCC*, San Antonio, TX, USA, Oct. 2014, pp. 1–10.

[14] M. Johns *et al.*, "Exploring shared control in automated driving," in *Proc. IEEE 11th ACM/IEEE Int. Conf. HRI*, Christchurch, New Zealand, Mar. 2016, pp. 91–98.

[15] C. Sentouh, S. Debernard, J. C. Popieul, and F. Vanderhaegen, "Toward a shared lateral control between driver and steering assist controller," *IFAC Proc. Volumes*, vol. 43, no. 13, pp. 404–409, 2010.

[16] S. M. Erlien, S. Fujita, and J. C. Gerdes, "Shared steering control using safe envelopes for obstacle avoidance and vehicle stability," *IEEE Trans. Intell. Transp. Syst.*, vol. 17, no. 2, pp. 441–451, Feb. 2016.

[17] K. Bengler, K. Dietmayer, B. Farber, M. Maurer, C. Stiller, and H. Winner, "Three decades of driver assistance systems: Review and future perspectives," *IEEE Intell. Transp. Syst. Mag.*, vol. 6, no. 4, pp. 6–22, Oct. 2014.

[18] S. K. Gehrig and F. J. Stein, "Collision avoidance for vehicle-following systems," *IEEE Trans. Intell. Transp. Syst.*, vol. 8, no. 2, pp. 233–244, Jun. 2007.

[19] S. J. Anderson, S. B. Karumanchi, and K. Iagnemma, "Constraint-based planning and control for safe, semi-autonomous operation of vehicles," in *Proc. IEEE Intell. Vehicles Symp.*, Madrid, Spain, Jun. 2012, pp. 383–388.

[20] S. M. Erlien, S. Fujita, and J. C. Gerdes, "Safe driving envelopes for shared control of ground vehicles," *IFAC Proc. Volumes*, vol. 46, no. 21, pp. 831–836, 2013.

[21] M. Brown, J. Funke, S. Erlien, and J. C. Gerdes, "Safe driving envelopes for path tracking in autonomous vehicles," *Control Eng. Pract.*, vol. 61, pp. 307–316, Apr. 2017.
[22] H. Okuda, N. Ikami, T. Suzuki, Y. Tazaki, and K. Takeda, "Modeling and analysis of driving behavior based on a probability-weighted ARX model," *IEEE Trans. Intell. Transp. Syst.*, vol. 14, no. 1, pp. 98–112, Mar. 2013.
[23] H. Okuda, X. Guo, Y. Tazaki, T. Suzuki, and B. Levedahl, "Model predictive driver assistance control for cooperative cruise based on hybrid system driver model," in *Proc. ACC*, Portland, OR, USA, Jun. 2014, pp. 4630–4636.
[24] T. Yamaguchi *et al.*, "Driver assistance control based on model predictive computation of constraint satisfaction," in *Proc. IEEE 18th Int. Conf. TSC*, Gran Canaria, Spain, Sep. 2015, pp. 1304–1310.
[25] N. Noto, H. Okuda, Y. Tazaki, and T. Suzuki, "Steering assisting system for obstacle avoidance based on personalized potential field," in *Proc. 15th Int. IEEE Conf. ITSC*, Anchorage, AZ, USA, Sep. 2012, pp. 1702–1707.
[26] F. Borrelli, P. Falcone, T. Keviczky, J. Asgari, and D. Hrovat, "MPC-based approach to active steering for autonomous vehicle systems," *Int. J. Veh. Auton. Syst.*, vol. 3, no. 2, pp. 265–291, 2005.
[27] K. Chen, B. Yang, X. Pei, and X. Guo, "Hierarchical control strategy towards safe driving of autonomous vehicles," *J. Intell. Fuzzy Syst*, vol. 34, no. 4, pp. 2197–2212, Apr. 2018.
[28] A. Koga, H. Okuda, Y. Tazaki, T. Suzuki, K. Haraguchi, and Z. Kang, "Realization of different driving characteristics for autonomous vehicle by using model predictive control," in *Proc. IEEE IV*, Gothenburg, Sweden, Jun. 2016, pp. 722–728.
[29] H. Okuda, Y. Liang, and T. Suzuki, "Sampling based predictive control with frequency domain input sampling for smooth collision avoidance," in *Proc. 21st Int. Conf. ITSC*, Maui, HI, USA, Nov. 2018, pp. 2426–2431.
[30] F. M. Verberne, J. Ham, and C. J. Midden, "Trust in smart systems: Sharing driving goals and giving information to increase trustworthiness and acceptability of smart systems in cars," *Hum. Factors*, vol. 54, no. 5, pp. 799–810, 2012.
[31] J. D. Lee, D. V. McGehee, T. L. Brown, and M. L. Reyes, "Collision warning timing, driver distraction, and driver response to imminent rear-end collisions in a high-fidelity driving simulator," *Hum. Factors*, vol. 44, no. 2, pp. 314–334, Jun. 2002.
[32] R. Sengupta, S. Rezaei, S. E. Shladover, D. Cody, S. Dickey, and H. Krishnan, "Cooperative collision warning systems: Concept definition and experimental implementation," *J. Intell. Transp. Syst.*, vol. 11, no. 3, pp. 143–155, Jul. 2007.

Keji Chen received the B.E. degree in vehicle engineering from the Wuhan University of Technology, Wuhan, China, in 2014, where he is currently pursuing the Ph.D. degree in vehicle engineering. From 2017 to 2019, he was a joint Ph.D. Student with the Graduate School of Engineering, Nagoya University, Japan. His research interests include vehicle dynamics, MPC, ADAS, and autonomous driving.

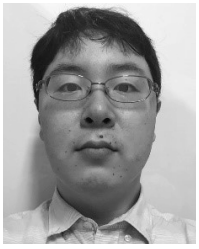

Takuma Yamaguchi was born in Aichi, Japan, in 1986. He received the Ph.D. degree from the Electronic Mechanical Engineering Department, Nagoya University, Japan. He is currently a Project Assistant Professor with Nagoya University. His research interests include probabilistic fault diagnosis, energy management systems, and applications of MPC. He is also a member of the SICE.

Hiroyuki Okuda (Member, IEEE) was born in Gifu, Japan, in 1982. He received the B.E. and M.E. degrees in advanced science and technology from the Toyota Technological Institute, Japan, in 2005 and 2007, respectively, and the Ph.D. degree in mechanical science and engineering from Nagoya University, Japan, in 2010.

He was a PD Researcher with the CREST, JST, from 2010 to 2012, and an Assistant Professor with the Nagoya University's Green Mobility Collaborative Research Center from 2012 to 2016. He was a Visiting Researcher with the Mechanical Engineering Department, University of California at Berkeley, in 2018. He is currently an Assistant Professor with the Department of Mechanical Science and Engineering, Nagoya University. His research interests are in the areas of system identification of hybrid dynamical system and its application to the modeling and analysis of human behavior and human-centered system design of autonomous/human–machine cooperative systems. He is a member of the IEEJ, SICE, and JSME.

Tatsuya Suzuki (Member, IEEE) was born in Aichi, Japan, in 1964. He received the B.S., M.S., and Ph.D. degrees in electronic mechanical engineering from Nagoya University, Japan, in 1986, 1988, and 1991, respectively.

From 1998 to 1999, he was a Visiting Researcher with the Mechanical Engineering Department, University of California at Berkeley. He is currently a Professor with the Department of Mechanical Systems Engineering and the Executive Director of the Global Research Institute for Mobility in Society, Nagoya University. He is also the Principal Investigator of JST, CREST. His current research interests are in the areas of analysis and design of human-centric mobility systems and integrated design of transportation and energy management systems. He is also a member of the SICE, ISCIE, IEICE, JSAE, RSJ, JSME, and IEEJ. He won the Best Paper Award at the International Conference on Autonomic and Autonomous Systems 2017, the Outstanding Paper Award from the International Conference on Control Automation and Systems 2008, and the Journal Paper Award from IEEJ, SICE, and JSAE in 1995, 2009, and 2010, respectively.

Xuexun Guo received the B.S. degree in power engineering from the Huazhong University of Science and Technology, Wuhan, China, in 1982, and the M.S. and Ph.D. degrees in vehicle engineering from the Beijing Institute of Technology, Beijing, China, in 1988 and 1995, respectively.

From 1982 to 1985, he was an Assistant Professor with the Department of Mechanic Engineering, Wuhan University. From 1995 to 2001, he was an Associate Professor with the School of Mechanical Science and Engineering, Huazhong University of Science and Technology. He has been a Professor with the School of Automotive Engineering, Wuhan University of Technology, since 2001. His research interests include hydraulic transmissions, brake systems, energy harvesting in vehicles, and electric vehicles.